# Mechanism Comparison for PAH Formation in Pyrolysis and Laminar Premixed Flames

W. Pejpichestakul[1], R. Tripathi[2], M. Pelucchi[1], L. Cai[2], H. Pitsch[2], E. Ranzi[1], T. Faravelli[*, 1]

[1]CRECK Modeling Laboratory, Department of Chemistry, Materials and Chemical Engineering "Giulio Natta", Politecnico di Milano, Italy

[2]Institute for Combustion Technology, RWTH Aachen University, Germany

**Abstract**

Polycyclic aromatic hydrocarbons (PAHs) are known precursors of harmful carbonaceous particles. Accurate predictions of soot formations strongly rely on accurate predictions of PAHs chemistry. This work addresses the detailed kinetic modeling of PAH formation using two models: CRECK [8] and ITV [12], aiming to compare the model predictions with experimental data in olefin pyrolysis and laminar premixed flames. The two kinetic mechanisms are validated and compared highlighting similarities and differences in PAHs formation pathways. The validation highlights the critical role of resonance-stabilized radicals leading to the PAH formation.

## Introduction

Combustion of hydrocarbon fuels is the main source of pollutants which causes adverse effects to the environment and human health. Combustion-generated polycyclic aromatic hydrocarbons (PAH) and soot particles are the main pollutants generated from burning of natural gas. Reducing pollutants emissions can be beneficiary not only for the environment and human health, but it can potentially increase the efficiency of combustion processes.

The first aromatic compound, benzene, is a key precursor of PAH and soot formation. It is formed mainly through the recombination of $C_2$, $C_3$ and $C_4$ molecules and radicals [1], via "odd" and "even" paths. Firstly, Miller and Melius [2] proved the notable role of the odd-carbon-atom pathways via the self-recombination of two propargyl radicals ($C_3H_3$•). Propargyl radical is a resonantly stabilized species, which is stable and present in a significant amount at high temperatures. The role of resonantly stabilized radicals (RSRs), such as propargyl and cyclopentadienyl ($C_5H_5$•), has been known as contributors to the successive PAH growth.

The "even" pathways move through successive additions of $C_2$ and $C_4$ species, with the initial benzene formation and the successive PAH growth, mostly because of acetylene addition (known as HACA - H-abstraction, acetylene addition) as proposed by Frenklach and co-workers [3].

Alkenes are components in hydrocarbon fuels and mainly key intermediates formed during the pyrolysis and combustion of the large alkyl chains in hydrocarbon and oxygenated fuels. Combustion of alkenes favorably forms allyl radicals, which are RSRs [4]. They can undergo PAH formation via addition and cyclization reactions.

This work presents a detailed kinetic modeling of PAH formation during the pyrolysis of propene and butene isomers in a flow reactor [4–6], as well as their combustion in a laminar premixed flame [7]. Two kinetic mechanisms including PAH formation, CRECK [8] and ITV[14], are used to compare model predictions against experimental data.

Pyrolysis experiments includes propene [4], 1- and 2-butene [5], as well as, isobutene [6] in a flow reactor at ~0.82 atm over a temperature range of about 800-1100 K. 50% fuel diluted in $N_2$ is fed with total flow rate of 30, 60 and 150 sccm in a 320 mm long tubular quartz reactor, with an internal diameter of 6 mm. The temperature profiles are measured axially along the length of the reactor, where the temperature in the center region is nearly constant. The constant temperature region corresponds to nominal residence times of 0.5-2.4 s. The models are also validated against a non-sooting premixed propene flame ($\phi$ = 2.3) at 50 mbar with a cold gas velocity of 48 cm/s [7].

## Numerical Method and Chemical Kinetics

The CRECK mechanism [8] consists of 244 species and approximately 6000 reactions. It implements a $C_0$-$C_3$ core mechanism obtained from the $H_2/O_2$ and $C_1/C_2$ subsets from Metcalfe et al. [9], $C_3$ from Burke et al. [10], and heavier fuels from Ranzi et al. [11]. It describes combustion of wide range hydrocarbon fuels and PAH formation up to $C_{20}$. The successive soot formation sub-mechanism is here neglected [8]. The ITV mechanism [12] consists of 369 species and 1896 reactions. It is built based on the $C_0$–$C_4$ model of Blanquart et al. [13] coupled with the aromatic combustion module from Narayanaswamy et al. [14] extended up to cyclopenta[cd]pyrene.

All numerical simulations were performed using OpenSMOKE++ suite by Cuoci et al. [15]. The measured temperature profiles were imposed to the simulations for most of the cases. Therefore, the energy equations were not solved. Concerning the premixed flame solver, the mixture-average diffusion coefficient was used in the simulation. Thermal diffusion (Soret effect) is also included in species transport equations.

* Corresponding author: tiziano.faravelli@polimi.it

**Results and Discussions**

The comparison of species profiles between experimental measurements and model predictions from CRECK and ITV mechanisms are presented here, starting with the pyrolysis of propene and butene isomers. Then, the results of the laminar premixed propene flame are discussed.

*Pyrolysis of propene*

Figure 1 compares predicted concentration profiles with the experimental data by Wang et al. [4] in propene pyrolysis at different residence times (0.5, 1.2, and 2.4 s). The CRECK model predicts the $C_3H_6$ conversion and major gaseous species quite satisfactorily at all residence times, while the ITV model shows a lower reactivity with a shifted temperature of ~80 K for all the species profiles. The decomposition of propene initially forms allyl ($C_3H_5$-A•) and H• radicals (R1), in both models. H• radical further enhances the decomposition through reaction (R2), which is a dominant pathway in fuel consumption and the formation of $C_2H_4$ and $CH_3$•. The addition reactions of allyl radical to propene with the successive cyclization to form five- and six-membered rings (reactions (R3) and (R4)), as well as, ethylene and 3-methyl-allyl (3-$C_4H_7$•) radical formation (R5), are very important primary reactions. These reactions, deeply discussed by Wang et al. [4], are missing in the ITV model and justify the lower reactivity.

While the ITV underpredicts all aromatic species due to its lower reactivity, the CRECK model underpredicts benzene ($C_6H_6$) and toluene ($C_7H_8$) concentration and slightly overpredicts the successive naphthalene formation at 1.2 and 2.4 s. The self-recombination of $C_5H_5$• radicals (R11) is the main route to naphthalene formation in both models.

At higher severity, i.e., at higher propene conversion, benzene is formed via the dehydrogenation reaction of cy$C_6H_8$ (R6). At these conditions, according to the CRECK model, cy$C_6H_8$ is formed not only through reaction (R4) but also through the $C_2H_2$ addition on $C_4H_6$. Propargyl addition on $C_4H_6$ (R7) is the dominant route to toluene ($C_7H_8$) formation. $C_4H_6$, which plays an important role in benzene and toluene formation, is formed via $C_2H_3$• addition on $C_2H_4$.

Concerning the ITV model, benzene is formed via the H-assisted isomerization of fulvene ($C_5H_4CH_2$) (R8), which is produced via $CH_3$• addition on $C_5H_5$•, and propargyl radical recombination (R9). $C_5H_5$• also has an important role in toluene formation through benzyl ($C_7H_7$•) radical via reaction (R10).

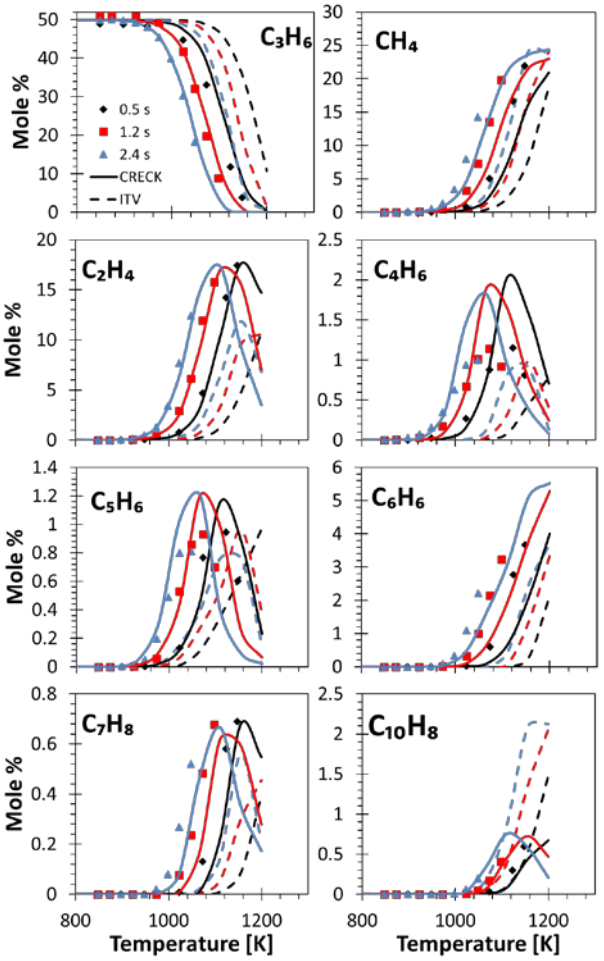


Figure 1 Comparison of model predictions (lines) and measurements (symbols) during propene pyrolysis [4].

$C_3H_6 = H• + C_3H_5\text{-}A•$ (R1)
$H• + C_3H_6 = CH_3• + C_2H_4$ (R2)
$C_3H_5\text{-}A• + C_3H_6 = CH_3• + cyC_5H_8$ (R3)
$C_3H_5\text{-}A• + C_3H_6 = H• + cyC_6H_8$ (R4)
$C_3H_5\text{-}A• + C_3H_6 = C_2H_4 + 3\text{-}C_4H_7•$ (R5)
$cyC_6H_8 = H_2 + C_6H_6$ (R6)
$C_3H_3• + C_4H_6 = H• + C_7H_8$ (R7)
$H + C_5H_4CH_2 = H + C_6H_6$ (R8)
$C_3H_3• + C_3H_3• = C_6H_6$ (R9)
$C_2H_2 + C_5H_5• = C_7H_7•$ (R10)
$C_5H_5• + C_5H_5• = 2H• + C_{10}H_8$ (R11)

*Pyrolysis of isobutene*

Figure 2 compares the species profiles between model predictions and experimental data [6] for isobutene pyrolysis. The CRECK model reasonably predicts the conversion of i-$C_4H_8$ and major species ($CH_4$ and $C_3H_6$) in the whole temperature range. Again, the ITV model underpredicts isobutene reactivity by~80 K. The chain initiation reaction of i-$C_4H_8$ (R12) forms H• and 2-methyl-allyl (i-$C_4H_7$•) radical, in both models, but the kinetic parameters are largely different. The following addition reaction of H• on i-$C_4H_8$ (R13) forms either the prevailing iso-butyl radical (i-$C_4H_9$•) or directly $C_3H_6$ and $CH_3$•. At low decomposition levels, the cycloaddition reactions of i-$C_4H_7$• radical on isobutene,

significantly contribute to the overall conversion in the CRECK model. Again, these reactions studied by Wang et al. [6] are not accounted for in the ITV model.

CRECK model overpredicts cyclopentadiene, whereas underpredicts methyl-cyclopentadiene and toluene, mainly at high decomposition levels. The self-recombination reaction of i-$C_4H_7$• radicals (R16) dominates toluene formation, together with the formation of dimethyl-cyclopentadiene ($C_7H_{10}$) (R15). The high concentration of i-$C_4H_7$• radical plays an important role in benzene formation also due to the addition to allene ($C_3H_4$-A) (R14). Together with the self-recombination of cyclopentadienyl radicals (R11), the addition of xylenyl radical ($C_8H_9$) on allene rules naphthalene formation (R17).

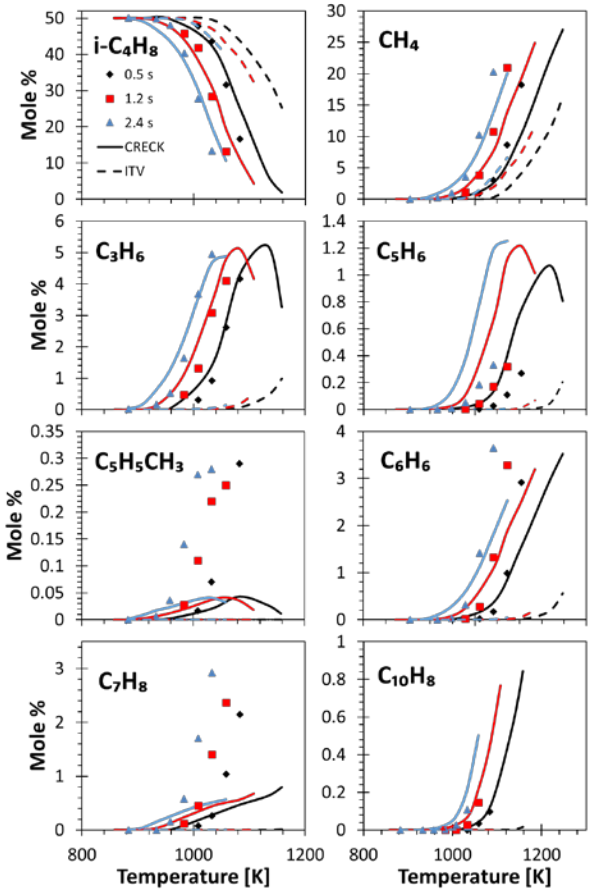


Figure 2 Comparison of model predictions (lines) and measurements (symbols) during isobutene pyrolysis [6].

| | |
|---|---|
| i-$C_4H_8$ = H• + i-$C_4H_7$• | (R12) |
| H• + i-$C_4H_8$ = $CH_3$• + $C_3H_6$ | (R13) |
| $C_3H_4$-A + i-$C_4H_7$• => $H_2$ + $CH_3$• + $C_6H_6$ | (R14) |
| i-$C_4H_7$• + i-$C_4H_8$ => $CH_3$• + $H_2$ + $C_7H_{10}$ | (R15) |
| i-$C_4H_7$• + i-$C_4H_7$• => H• +$H_2$ + $CH_3$• + $C_7H_8$ | (R16) |
| $C_3H_4$-A + $C_8H_9$• => $H_2$ + $CH_3$• + $C_{10}H_8$ | (R17) |

*Pyrolysis of 1-butene*

Figure 3 shows the comparison of species profiles between model predictions and experimental data [5] during 1-butene pyrolysis as a function of temperature at different residence times. The CRECK model shows a lower 1-butene reactivity, while the ITV model correctly captures the decomposition extent. Despite the underpredictions of the concentration of most species, the CRECK model overpredicts toluene formation, because of a higher addition of methyl-allyl radicals on butene. The ITV model slightly overpredicts $C_3H_6$ and $C_{10}H_8$ while underpredicts the remaining species.

The initiation reaction of 1-butene forms $CH_3$• and $C_3H_5$-A• (R18). In the CRECK model, $C_3H_6$ and $CH_3$• are mainly formed via a chemically activated pathway of H• addition on 1-butene (R20), while H• addition and on 1-butene forming 1-$C_4H_9$ prevails in the ITV model (R19).

In the CRECK model, the dehydrogenation reaction (R6) largely contributes to benzene formation, and $cyC_6H_8$ is initially formed via the cycloaddition of methyl-allyl radical on 1-butene and then by the addition of vinyl radical on $C_4H_6$. Reaction (R21) plays a major role in the formation of toluene. The $C_4H_6$ addition on benzene (R22), as well as, similar cycloaddition reactions of $C_4$ species on the aromatic ring, lead to the formation of naphthalene, always together with the $C_5H_5$• radical recombination (R11).

On the other hand, the ITV model predicts benzene formation via reaction (R8), toluene formation via (R10), and naphthalene through reaction (R11).

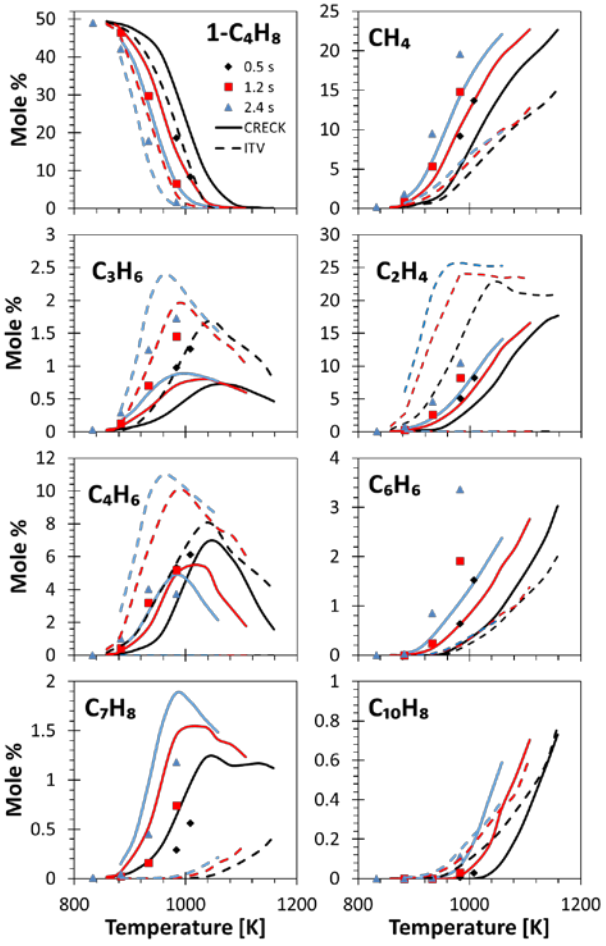


Figure 3 Comparison of model predictions (lines) and measurements (symbols) during 1-butene pyrolysis [5].

$1\text{-}C_4H_8 = CH_3\bullet + C_3H_5\text{-}A\bullet$ (R18)
$H\bullet + 1\text{-}C_4H_8 = 1\text{-}C_4H_9\bullet$ (R19)
$H\bullet + 1\text{-}C_4H_8 = CH_3\bullet + C_3H_6$ (R20)
$3\text{-}C_4H_7\bullet + C_4H_6 => H_2 + CH_3\bullet + C_7H_8$ (R21)
$C_4H_6 + C_6H_6 => 2H_2 + C_{10}H_8$ (R22)

*Pyrolysis of 2-butene*

The results for 2-butene pyrolysis are only limited to the CRECK model, as this species is only considered as an intermediate product in the ITV model. Fuel conversion and the major products ($CH_4$, $C_2H_4$, $C_3H_6$, and $C_4H_6$) are reasonably predicted. On the contrary, benzene and naphthalene concentrations are underpredicted, whereas toluene concentration is overpredicted at all temperatures and residence times.

Initially, 2-butene isomerizes to form 1-butene, but the dominant pathway in 2-butene conversion is H-assisted decomposition (R23) forming $CH_3\bullet$ and $C_3H_6$, which is the main route giving $C_3H_6$. Again, $CH_4$ is mainly formed via $CH_3\bullet$ addition and abstraction on 2-butene. The dehydrogenation of $cyC_6H_8$ reaction (R6) largely forms benzene, whereas $cyC_6H_8$ is formed through the cycloaddition of $3\text{-}C_4H_7\bullet$ and 2-butene (R24). Due to its high concentration, $3\text{-}C_4H_7\bullet$ radicals can add on butenes and $C_4H_6$ (R21) leading $C_7H_8$, together with the recombination of $3\text{-}C_4H_7\bullet$ (R25). Similar to 1-butene, reactions (R11) and (R22) lead to the formation of naphthalene.

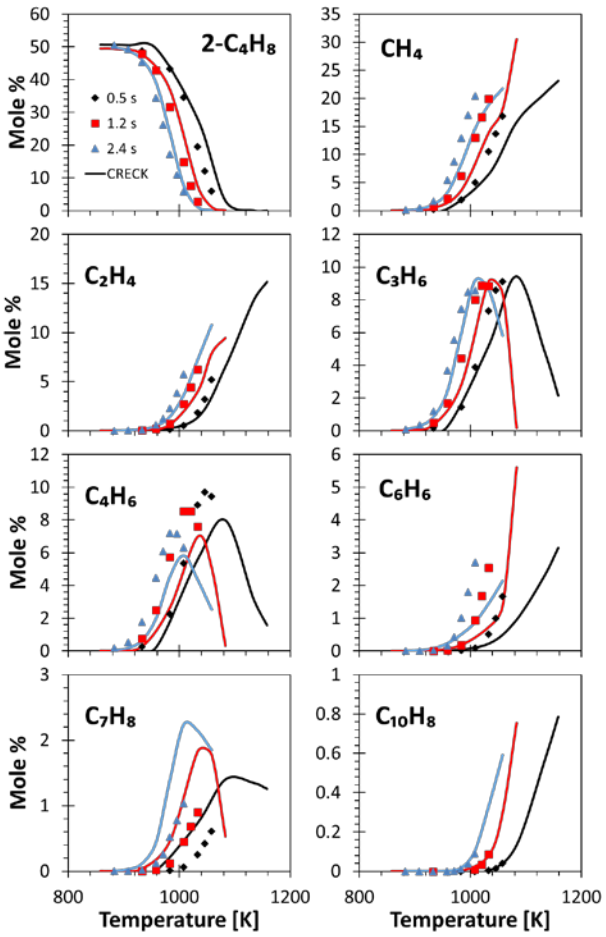


Figure 4 Comparison of model predictions (lines) and measurements (symbols) during 2-butene pyrolysis [5].

$H\bullet + 2\text{-}C_4H_8 = CH_3\bullet + C_3H_6$ (R23)
$2\text{-}C_4H_8 + 3\text{-}C_4H_7\bullet => H_2 + C_2H_5\bullet + cyC_6H_8$ (R24)
$3\text{-}C_4H_7\bullet + 3\text{-}C_4H_7\bullet => H_2 + CH_3\bullet + C_7H_8$ (R25)

All these data and comparisons of olefin pyrolysis clearly highlight the impact of allyl and methyl-allyl resonantly stabilized radicals, which are readily formed and accumulate in the reacting system, thus reaching high concentrations. The fuel structure is an important factor, which controls the radical pool inside the system leading to different product distributions. These differences result in different initial pathways in PAH formation, whereas there is a successive and progressive convergence towards more similar and asymptotic thermodynamic conditions.

The primary radical formed during the fuel decomposition proves to be the crucial species undergoing PAH formation because of the cycloaddition occurring initially on parent fuels and then on unsaturated intermediate species. The self-recombination of primary radicals is also relevant. Nevertheless, the PAH formation process through the cycloaddition reactions of RSRs is a multi-step process, often lumped and simplified. In fact, it can require addition with successive isomerization, cyclization, H-transfer, dehydrogenation, and β-scission reactions. The important role of butadiene

and allene is also observed, mainly in the initial growth of PAH species as they feature resonant intermediate products preventing the back-dissociation to reactants.

The relevant role of the resonant $C_3H_3$• and $C_5H_5$• radicals in the formation of PAH is well recognized, in both ITV and CRECK models. The self-recombination of $C_3H_3$• radicals is one key reaction promoting the initial benzene formation. Additionally, the $CH_3$• addition on $C_5H_5$• gives fulvene, which readily isomerizes to benzene.

*Premixed propene/oxygen/argon flame*

Figures 5 compares the concentration between the experimental data and the models [7] along the height above the burner (HAB). CRECK and ITV models satisfactorily capture the mole fraction of fuel quite well, however, both models slightly underpredict the $O_2$ at the region close to the burner due to the overpredictions of $H_2$. The CRECK model slightly overpredicts $H_2O$ leading to a small underestimation of $CO_2$. The ITV model estimates the higher concentration of $H_2O$ and $CO_2$ in comparison with the CRECK model resulting in a lower CO mole fraction. Both models can capture the major oxidation products quite well. In spite of the good agreement observed for $C_2H_4$ with the CRECK model, $C_2H_2$ is overestimated particularly in the post-flame region. The ITV model slightly underestimates the $C_2H_4$ mole fraction, which subsequently leads to the overprediction of $C_2H_2$. The CRECK model underpredicts both $C_3H_4$ (allene and propyne) and propargyl radical concentrations, leading to the underpredictions of aromatic species, although the previous CRECK model [16] shows good propargyl and aromatic species yields. This difference is due to the update of $C_0$-$C_3$ core, which requires further assessments of pressure-dependent rate parameters. The ITV model provides good predictions for $C_3$ species. However, both models predict a higher concentration of propyne ($C_3H_4$-P) compared to allene. The ITV model captures the concentration of most aromatic species well, while underpredicting indene. However, the good prediction of the ITV mechanism for low pressure flame may come from error compensation, as the ITV mechanism does not incorporate pressure-dependent rate constants at low pressures.

For the CRECK model, at the HAB = 0.5, $C_3H_6$ decomposes to form $C_2H_4$ via reaction (R26) and it is also abstracted forming $C_3H_5$-A•. Vinyl ($C_2H_3$•) radical mostly is formed via the H-abstraction of $C_2H_4$, in which $C_2H_3$• produces $C_2H_2$ and H• (R27). In the ITV model, $C_2H_4$ is formed via reaction (R28), where $C_2H_5$• is formed through $CH_3$• recombination (R29) and dehydrogenation. The CRECK model predicts propyne formation via the dehydrogenation of propene, whereas $C_3H_3$• is formed via (R30). For the ITV model, $C_3H_5$-A• forms H• and $C_3H_4$-A, which quickly isomerizes to $C_3H_4$-P. The subsequent H-abstraction by H• produces $C_3H_3$•.

The dominant pathway in benzene formation is the recombination of propargyl radical (R9), followed by the isomerization of fulvene for both models. However, fulvene isomerization is supported by H• (R8) in the ITV model, while in the CRECK model, it occurs via reaction (R31). Toluene is formed from benzyl radical via reaction (R32) in CRECK, whereas it is directly produced through reaction (R33) in the ITV model. $CH_3$• addition on indenyl ($C_9H_7$•) radicals (R35) lead to naphthalene formation in the ITV model. The same reaction is missing in CRECK model. Therefore, naphthalene is formed via the recombination of propargyl and benzyl radicals (R34). Both CRECK and ITV models predict indene ($C_9H_8$) formation through propargyl addition on phenyl ($C_6H_5$•) radicals (R36).

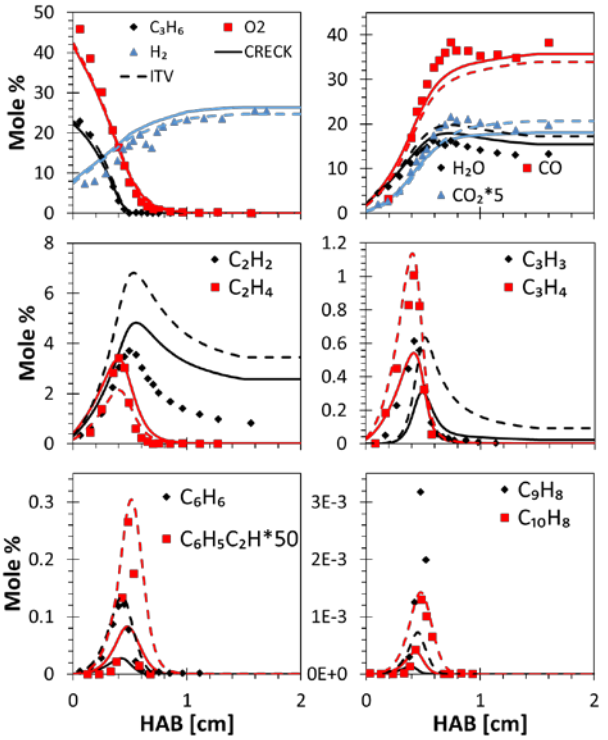


Figure 5 Comparison of model predictions (lines) and measurements (symbols) in premixed propene flame [7].

$H• + C_3H_6 = CH_3• + C_2H_4$ (R26)
$C_2H_3• = H• + C_2H_2$ (R27)
$C_2H_5• = H• + C_2H_4$ (R28)
$CH_3• + CH_3• = H• + C_2H_5•$ (R29)
$C_4H_6 = CH_3• + C_3H_3•$ (R30)
$C_5H_4CH_2 = C_6H_6$ (R31)
$H• + C_7H_7 = CH_3• + C_6H_5•$ (R32)
$CH_3• + C_6H_5• = C_7H_8$ (R33)
$C_3H_3• + C_7H_7• = 2H• + C_{10}H_8$ (R34)
$CH_3• + C_9H_7• = 2H• + C_{10}H_8$ (R35)
$C_3H_3• + C_6H_5• = C_9H_8$ (R36)

The good predictive capabilities of the ITV model highlights that the important reactions controlling pyrolysis do not play a role at flame conditions. Therefore, the comparisons using CRECK and ITV models is an important step toward the unification of PAH mechanisms, in addition to the need of a unified core mechanism, as implemented in the CRECK model

(i.e. Aramco 2.0). The case study here motivates the future improvement of the kinetic models and a deeper understanding of PAHs growth kinetics.

## Conclusions

The kinetic study of olefins pyrolysis and combustion has been carried out in a flow reactor and laminar premixed flames using CRECK and ITV models. The pyrolysis of olefins including propene and 3 butene isomers was performed at isothermal conditions in the temperature range of about 800-1100 K. Model predictions of fuel conversion, concentration profiles of major small gaseous and aromatic species were compared with the experimental data as a function of temperature at three different residence times. The residence times reported here correspond to the effective residence time in the nearly constant temperature region in the flow reactor. The validation of low-pressure premixed propene flames was also performed to study the dominant pathway in PAH formation at high temperature. The simulations were carried out using the measured temperature profile with a maximum temperature of ~2300 K.

The CRECK model reasonably captures fuel conversion and gaseous species profiles, as well as, PAHs formation in most pyrolysis conditions. The model demonstrates the role of the primary allylic radicals formed during the fuel decomposition in promoting major gaseous and PAH products. The dominant PAH formation pathways under these conditions are those involving RSRs via the initial addition of primary allylic radicals to parent fuels and the addition to intermediate unsaturated species, as well as its recombination. However, underpredictions of $C_3$ species were observed in flame, which leads to the underprediction in PAHs. These discrepancies in $C_3$ species predictions are related to the pressure-dependent rate in forming $C_3H_4$ isomers. Therefore, further investigation is required.

The ITV model predicts the concentration profiles under low-pressure propene flames quite well, although an overprediction is observed for acetylene. The model well captures propargyl and $C_3H_4$ concentration leading to good predictions of PAH concentrations. However, the model has slow reactivity during pyrolysis of propene and butene isomers in most conditions, except 1-butene pyrolysis, due to the absence of the addition of primary radical on parent fuels. The temperature shift of ~80 K is observed in the pyrolysis of propene and isobutene. The dominant pathways in aromatic species mostly involve $C_3H_3$• and $C_5H_5$•.

The predictions using CRECK and ITV models show common key pathways of fuel decomposition. However, the dominant reactions leading to PAH formation show some important differences, especially under pyrolysis conditions. This comparison allows the detailed kinetic study of PAH formation with the aim to join the efforts and arrive to a common mechanism able to improve the performances of the kinetic models and the understanding of PAHs growth kinetics.


## Acknowledgments

This work is supported by The Computational Chemistry Consortium (C3).


## References


[1] H. Wang, M. Frenklach, Combust. Flame 2180 (1997) 173–221.

[2] J.A. Miller, C.F. Melius, Combust. Flame 91 (1992) 21–39.

[3] M. Frenklach, D.W. Clary, W.C. Gardiner, S.E. Stein, Symp. Combust. 20 (1985) 887–901.

[4] K. Wang, S.M. Villano, A.M. Dean, Combust. Flame 162 (2015) 4456–4470.

[5] K. Wang, S.M. Villano, A.M. Dean, Combust. Flame 173 (2016) 347–369.

[6] K. Wang, S.M. Villano, A.M. Dean, Combust. Flame 176 (2017) 23–37.

[7] H. Böhm, A. Lamprecht, B. Atakan, K. Kohse-Höinghaus, Phys. Chem. Chem. Phys. 2 (2000) 4956–4961.

[8] W. Pejpichestakul, E. Ranzi, M. Pelucchi, A. Frassoldati, A. Cuoci, A. Parente, T. Faravelli, Proc. Combust. Inst. 37 (2018) 1013–1021.

[9] W.K. Metcalfe, S.M. Burke, S.S. Ahmed, H.J. Curran, Int. J. Chem. Kinet. 45 (2013) 638–675.

[10] S.M. Burke, U. Burke, R. Mc Donagh, et al., Combust. Flame 162 (2015) 296–314.

[11] E. Ranzi, a. Frassoldati, R. Grana, A. Cuoci, T. Faravelli, A.P.P. Kelley, C.K.K. Law, Prog. Energy Combust. Sci. 38 (2012) 468–501.

[12] K. Narayanaswamy, H. Pitsch, P. Pepiot, Combust. Flame 162 (2015) 1193–1213.

[13] G. Blanquart, P. Pepiot-Desjardins, H. Pitsch, Combust. Flame 156 (2009) 588–607.

[14] K. Narayanaswamy, G. Blanquart, H. Pitsch, Combust. Flame 157 (2010) 1879–1898.

[15] A. Cuoci, A. Frassoldati, T. Faravelli, E. Ranzi, Comput. Phys. Commun. 192 (2015) 237–264.

[16] A. Frassoldati, T. Faravelli, E. Ranzi, K. Kohse-Höinghaus, P.R. Westmoreland, Combust. Flame 158 (2011) 1264–1276.